



Polymer Communication

Corona discharge from electrospinning jet of poly(ethylene oxide) solution

Sureeporn Tripatanasuwan, Darrell H. Reneker*

Department of Polymer Science, The University of Akron, 170 University Ave., Akron, OH 44325, USA

ARTICLE INFO

Article history:

Received 17 October 2008

Received in revised form

3 February 2009

Accepted 7 February 2009

Available online 24 February 2009

Keywords:

Electrospinning

Poly(ethylene oxide)

Corona discharge

ABSTRACT

Corona discharges from electrospinning jets were observed and photographed at the tip of the Taylor cone, and in a cylindrical region around the jet, a few millimeters below the tip. The corona discharge was also faintly visible to a dark adapted eye. At the position at which the cylindrical corona discharge became apparent, typical conditions were a jet diameter of 30 μm , an applied potential of 12 kV, and a calculated radial electric field of 400 kV/cm. The calculated electric field required to create a corona in air around a metal wire of the same diameter, calculated from Peek's empirical formula, was only about 200 kV/cm. The cross sectional shape of some segments of the electrospun fibers had two or three lobes. The lobes often separated, and formed smaller fibers.

© 2009 Elsevier Ltd. All rights reserved.

1. Introduction

Electrohydrodynamical jets, of the sort used in the electrospinning of nanofibers, are known to be affected by the airborne ions created by corona discharges [1]. The development of beaded fibers [2] is an example. Recently it was shown that current flowing through the air, from the region surrounding the jet to a ground collector, reduced the surface charge density and increased lateral stability of a jet [3].

This paper describes the photography of the light from the corona discharges that occur during electrospinning. The location and intensity of the corona are recorded in relation to the path of the charged jet. Corona discharges were observed primarily near the tip of the Taylor cone, and around the flowing jet. These incisive observations make it possible to see the corona wherever it occurs. The corona can then be avoided or used as a control parameter for the electrospinning process. Differences in the behavior of the corona for jets charged to positive and negative potentials were noted.

Experimental and theoretical descriptions of electrospinning were published by Reneker and Yarin [4,5]. The electric field near the jet depends primarily on the electrical potential, and the radius of the curvature of the jet or the surface of the Taylor cone. If the electric field at the surface of the Taylor cone or the jet exceeded a critical value, a corona discharge was observed to occur. The observed electric field required to create a corona discharge near

a thin jet or a thin metal wire is 5 or 10 times higher than the electric field required to create a centimeter long spark in air.

2. Experiment

An aqueous solution of 6% poly(ethylene oxide) with molecular weight of 400,000 was held in a glass pipette. The electrical potential of the solution was adjusted by electrons flowing through a metal wire inserted into the solution. In separate experiments, either a negative or a positive electrical potential was applied between the solution and the metal collector plate. A sensitive video camera (0.0001 lux) was used at a rate of 30 frames per second. The exposure time was controlled by the camera, but less than 30 ms. The region where the corona occurred, in the vicinity of a Taylor cone or jet, was imaged. A repeated short flash (around 100 μs) illuminated the tip and the path of the jet in about every fifth frame, so that the corona discharge, the jet, and the tip of the glass pipette, were seen clearly in one image.

3. Results and discussions

Fig. 1 shows a corona discharge near the tip of the Taylor cone before the jet formed. A negative potential difference of 25 kV was applied between the droplet and a metal plate 150 mm below the droplet.

After the jet formed, a corona discharge was observed when the negative electrical potential between the tip and metal plate exceeded 5 kV. The corona typically began about 1 or 2 mm below the tip and extended for about 1 mm along the jet. The corona was faintly visible in a dark room. In the same experimental

* Corresponding author. Tel.: +1 330 294 6949; fax: +1 330 294 5290.
E-mail address: reneker@uakron.edu (D.H. Reneker).

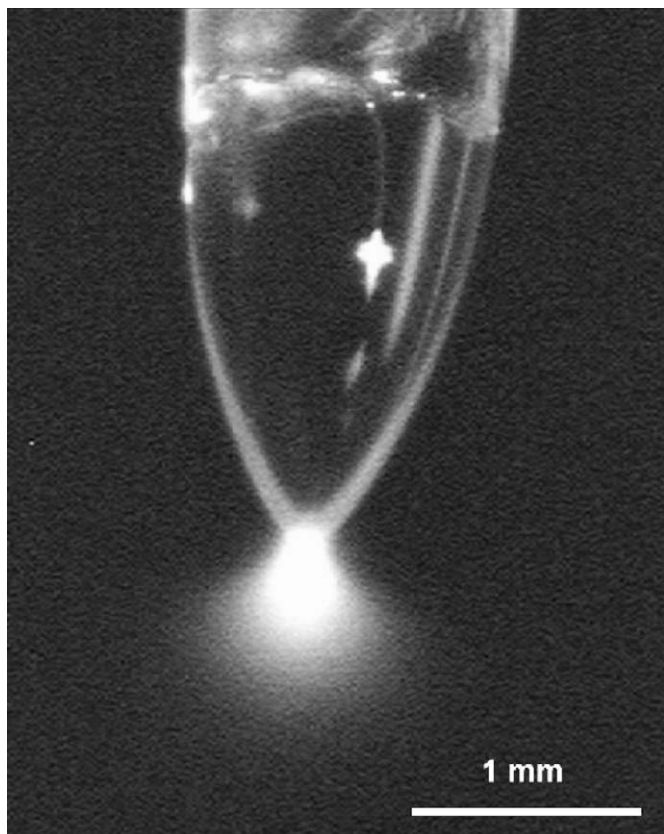


Fig. 1. Corona discharge from tip of the Taylor cone.

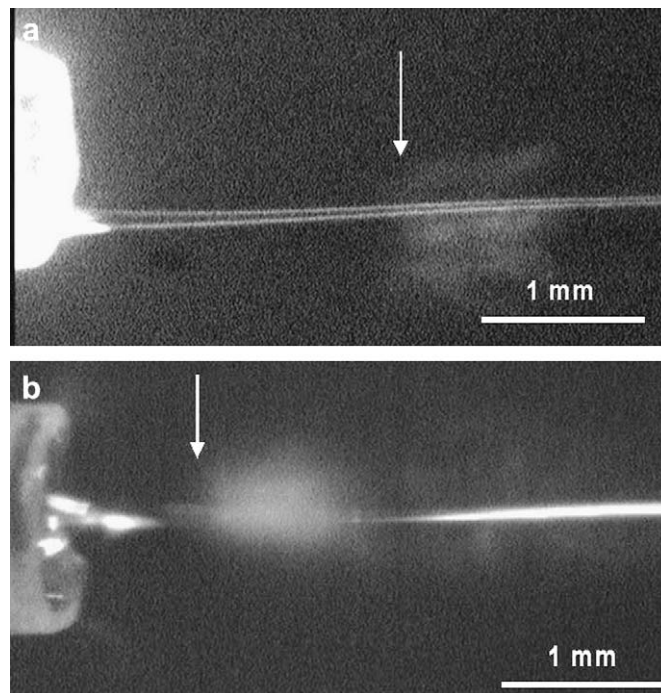


Fig. 2. Corona discharge from a negatively charged jet of poly(ethylene oxide) solution. The applied potential between tip and a metal plate placed 45 mm below the tip was (a) 12 kV and (b) 20 kV. The white arrows show the position along each jet at which the corona became visible. The exposure of the jet was dominated by the duration of the flash, while the light from the corona was integrated over the exposure time per frame, which was less than 30 ms.

arrangement, but with a positive potential at the tip, the onset of the corona along the jet began at a potential of 10 kV. The light from the corona became more intense when the electrical potential, of either polarity, increased.

Fig. 2(a) shows a negative jet at a potential of 12 kV. The position along the jet at which the corona became visible is marked with a white arrow. The measured radius of the jet at this position was $30 \pm 5 \mu\text{m}$.

In Fig. 2(b) the negative potential was 20 kV. The radius of the jet was not measured. The variation, of the specularly reflected light along the jet, as shown in Fig. 2(b), indicates that the jet was often slightly curved in the region where the corona was observed, at the instant that the flash occurred.

To calculate the radial electric field, the charged jet and its surroundings were approximated as a cylindrical capacitor. The zero potential was assigned to a hypothetical outer metal cylinder with a radius A , of 10 cm. The radius of the outer cylinder was chosen to be equal to the radial distance from the jet to the nearest part of the metal support structure, which was also at zero potential with respect to the collector. The value of the radius of the hypothetical cylinder was large enough that an assumption of a larger radius would contribute little change to the calculated value of the electric field at the surface of the jet.

The radial component of electric field between the concentric cylinders is given by

$$E = \varphi_0 / [r \ln(A/a)]$$

where φ_0 is the potential applied between the central cylinder and the grounded outer cylinder. The electric field at the surface of the jet, where $r = a$, is:

$$E = \varphi_0 / [a \ln(A/a)]$$

The radius of the jet was measured at the place where the corona discharge became visible. The surface potential of the jet was assumed to be maintained at φ_0 by the ionic conductivity of the solution, which was about $1.48 \times 10^{-4} \text{ S/cm}$. The electrical relaxation time, (dielectric constant divided by conductivity) of the aqueous solution was about $4.7 \times 10^{-8} \text{ s}$, during which time the change in the shape of the jet was small. This indicates the implicit assumption that the surface of the jet is an equipotential surface is useful up to the corona region.

The radial component of electric field at the surface of the jet increased, as the radius of the tapering jet decreased with distance from the tip. The onset of the corona discharge was observed to occur when the jet radius was $30 \pm 5 \mu\text{m}$, as shown in Fig. 2(a), when the applied potential was 12 kV. The radial electric field calculated from the above formula was around 400 kV/cm, which can be compared to the electric field at which a corona discharge occurs around an electrically conducting metal cylinder.

The electric field required to initiate a corona discharge around a metal wire can be estimated from Peek's empirical equation [6], $E_c = 30 \delta [1 + 0.3/(\delta r)]^{1/2}$, where E_c is the electric field for onset of corona in kV/cm, δ is an air density factor that is near one at ambient conditions, and r is the radius of the wire in centimeters. Peek's equation was used successfully to describe the onset of corona discharge around a wire in recent papers [7,8]. A negative-corona discharge in oxygen at a hyperboloidal electrode was modeled by Zhang et al. [9]. For a metal wire with a radius of $30 \pm 5 \mu\text{m}$, which is the radius of the jet at the beginning of the corona discharge shown in Fig. 2(a), the predicted electric field from Peek's equation for the onset of corona on a wire was around $200 \pm 15 \text{ kV/cm}$, about half the field calculated from the observed onset voltage for a jet of the same diameter.

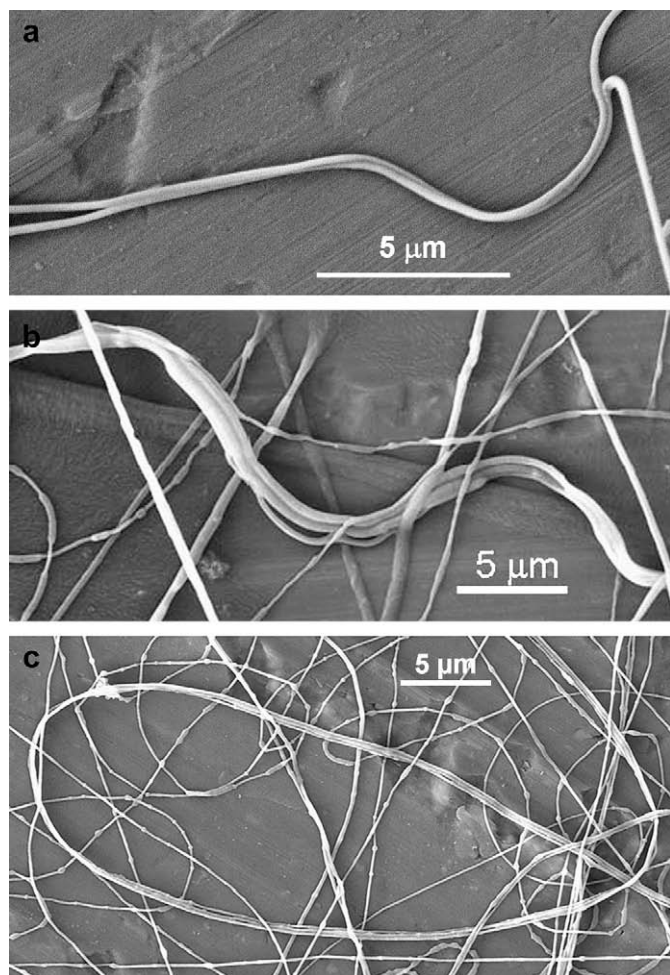


Fig. 3. (a) A single fiber with two lobes separated by a groove. The lobes separated into two fibers at each end of the segment. The tip voltage was negative 30 kV. (b) A fiber segment with three lobes that split into three fibers near the center of the figure. The tip voltage was negative 15 kV. (c) A fiber segment that formed a large loop. The edge on view at the right and left sides of the loop show that the segment has a ribbon-like character. Short, separated fiber segments are visible. Multiple lobes are rarely observed in polyethylene oxide fibers electrospun at lower potentials. This figure also shows typical side by side interactions between segments. The distance over which the side by side fibers are parallel is typically much shorter than the lengths of the multilobal fibers. The tip voltage was positive 30 kV.

Reduction of charge per unit area on the surface of the jet, by the loss of the charge that produced the corona, reduced the radial electric field to a value that did not sustain the corona discharge. In Fig. 2, the observed corona discharge extended for only about 1 mm along the jet, and about 0.5 mm in the radial direction.

At a greater distance from the tip, the straight segment of the jet path changed to an electrical bending coil [4]. Electrospun fibers were collected on a flat sheet, about 150 mm below the tip. Fig. 3 shows scanning electron micrographs of the electrospun fibers that

were collected. Fibers with 2 or 3 lobes that split into 2 or 3 fibers are abundant in these images, but uncommon in the nanofibers electrospun from polyethylene oxide solutions at lower voltages. Split fibers of hydroxyethylmethacrylate were also reported by Koombhongse et al. [10]. A web between lobes in a bilobal fiber, observed in some fibers, indicates that a skin formed on the jet and collapsed as the jet solidified.

4. Conclusions

The onset of a corona discharge in air occurred when the radial electric field near the jet, calculated for a conductor of the same diameter at the center of a coaxial capacitor, was higher than the field required to establish a corona around a metal wire of the same diameter, estimated from Peek's formula. The corona discharge current reduces both the charge per unit area on the surface of the jet and the radial electric field, to values that do not sustain the corona discharge. Simulations [11] in the context of mass spectroscopy, called to our attention by a reviewer, indicate that both droplet fission and ion evaporation take place in electrosprays. Closely related phenomena are certainly involved in electrospinning, and their possible effects, on parameters such as surface tension, skin formation, and surface tension, need to be examined. The radial electric field at the surface of the jet is much higher than the value of the electric field at which a spark forms between centimeter scale metal spheres in air, which is about 30 kV/cm. Observations of corona discharges offer new tools for the improvement of the electrospinning process.

Acknowledgement

This work was supported by NSF NIRT grant, #DMI-0403835 and NSF 1110-0038-002. Support and guidance from the Coalescence Filtration Nonmaterial Consortium is acknowledged. Consortium members are the Donaldson Company, Ahlstrom Turin, Parker-Hannifin, Hollingsworth and Vose, and Cummins Filtration.

References

- [1] Filatov Y, Budka A, Kirichenko V. *Electrospinning of micro- and nanofibers: fundamentals and applications in separation and filtration processes*. New York: Begell House; 2007. p. 48.
- [2] Fong H, Chun I, Reneker DH. *Polymer* 1999;40(16):4585–92.
- [3] Korkut S, Saville DA, Aksay IA. *Physical Review Letters* 2008;100(3):034503.
- [4] Reneker DH, Yarin AL. *Polymer* 2008;49(10):2387–425.
- [5] Reneker DH, Yarin AL, Zussman E, Xu H. *Advances in Applied Mechanics* 2007;41:43–195.
- [6] Peek FW. *Dielectric phenomena in high voltage engineering*. New York: McGraw-Hill; 1929. p. 42.
- [7] Lowke JJ, D' Alessandro F. *Journal of Physics D: Applied Physics* 2003;36(21):2673–82.
- [8] Dumitran LM, Dascalescu L, Atten P, Notingher PV. *IEEE Transactions on Industrial Applications* 2002;42(2):377–84.
- [9] Zhang J, Adamiak K, Castle GSP. *Journal of Electrostatics* 2007;65(3):174–81.
- [10] Koombhongse S, Liu W, Reneker DH. *Journal of Polymer Science Part B Polymer Physics* 2001;39(21):2598–606.
- [11] Luedtke WD, Landman U, Chiu YH, Levandier DJ, Dressler RA, Sok S, et al. *Journal of Physical Chemistry A* 2008;112(40):9628–49.